

CHAPTER IV

RESULTS AND DISCUSSION

4.1 The characterization of clays

Raw bentonite was kindly provided by Cernic International Co., Ltd. Prior to use, it was preliminarily characterized by X-ray diffraction (XRD). X-ray diffraction is the most important tool for the qualitative analysis of clay mineral samples by following the changes in the position and the intensity of d_{001} reflection. It is easy and fast to carry out and provides a large amount of information.

4.1.1 The characterization of raw bentonite by XRD

Natural clay is not composed of one clay mineral only. Bentonite is an aluminum phyllosilicate clay, generally and mostly impured by quartz. Impurities such as calcite, quartz, feldspars and humic acids are most common components in addition to the pure clay mineral. Quartz is the major component in rocks and minerals. Crystallized as large three-dimensional network grains, quartz has low surface area and acidic site, which interrupts the analysis of clays. The characteristic structure of raw bentonite was analyzed by XRD technique as shown in Fig. 4.1.

XRD pattern of raw bentonite is shown in Figure 4.1. The characteristic peaks of bentonite were detected at 2-theta range about 7 and 19 degree. The main crystalline impurity was quartz (SiO_2), which gave the sharp peak at 26.6 degree.

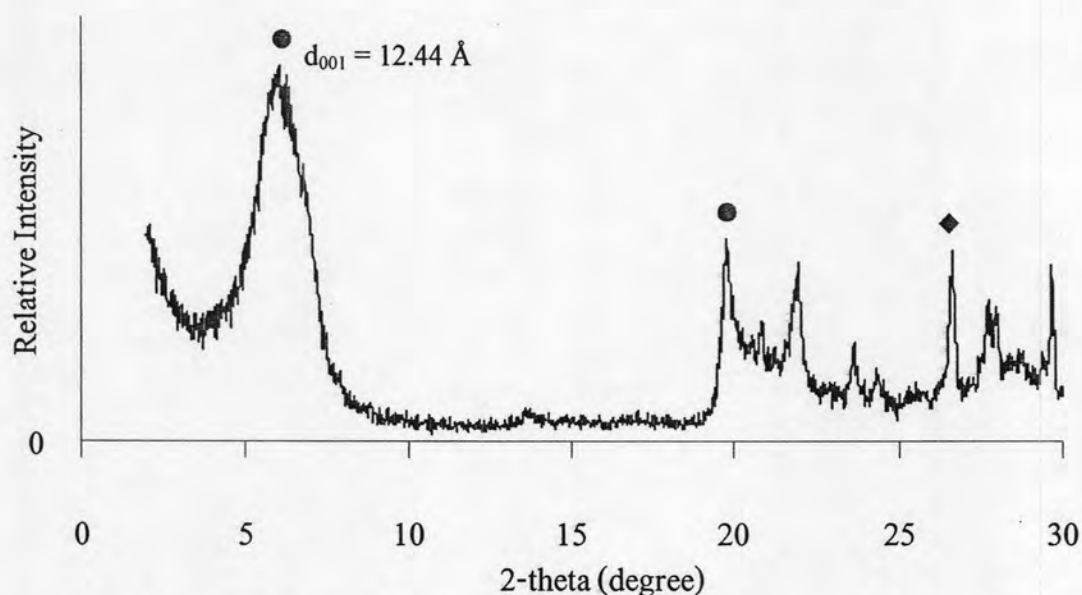


Figure 4.1 XRD pattern of raw material bentonite (● represents bentonite peaks and ◆ represents impurity quartz peak).

4.2 The synthesis and characterization of homoionic clays

Homoionic bentonite was prepared by purification and ion exchange method [40]. In the purification process, quartz and other impurities were removed from bentonite by centrifugal technique. The Na ion is preferred to intercalate between the clay layers in order to obtain homoionic clays before further modification. The resulting products are white powder, used as the starting materials.

4.2.1 Purification of bentonite

Bentonite swells with the addition of water. Its volume expands considerably more than other clays due to water penetrating the interlayer molecular spaces and concomitant adsorption. Raw bentonite contains quartz and other impurities. These impurities could be removed by repetitive dispersion and centrifugation approach.

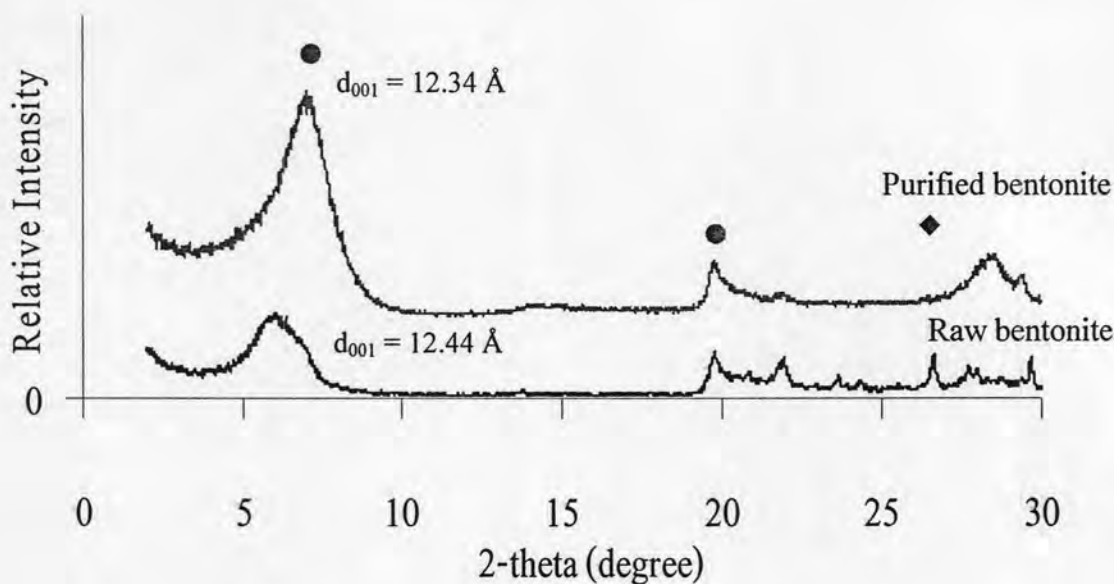


Figure 4.2 XRD patterns of raw bentonite and Na-bentonite. XRD patterns of raw bentonite and purified bentonite obtained at the centrifugal speed of 4000 rpm (represents bentonite peaks and represent impurity quartz peak).

The XRD patterns of the raw material and purified bentonite are shown in Fig. 4.2. The quartz peak disappeared in purified bentonite collected from the centrifugal speed of 4000 rpm, suggesting quartz and other crystalline impurities were removed from raw bentonite. Because of the large grain size of quartz, its sediments were collected and separated at lower centrifugal speed of 2000 rpm beforehand. In addition, any water-soluble impurity was supposed to be removed during the process. Purified bentonite shows the d_{001} spacing in the range of 12 to 13 Å. The XRD pattern still remains the characteristic pattern of bentonite.

4.2.2 Na-ion exchange

X-ray diffraction of Na-bentonite

Depending on the composition of the tetrahedral and octahedral sheets, the layer has either no charge or a net negative charge. If the layers are charged this charge is balanced by interlayer cations such as Na^+ or K^+ . In each case the interlayer can also contain water. The amount of expansion is due largely to the type of exchangeable cation contained in the sample. The presence of sodium as the predominant exchangeable cation can result in the clay swelling to several times its original volume, due to the large solvation energy of Na^+ and its small electrostatic interaction between monovalent cations and negatively layered charge. Thus, Na-ion

exchange was necessary to expand the interlayer distances. Bentonite treated with 5 M NaOH for three times, was chosen as starting homoionic clay and designated as Na-bentonite. The XRD patterns of purified bentonite and Na-bentonite are compared in Fig 4.3. The d_{001} spacing of Na-bentonite was higher than that of the untreated one suggested that Na ions intercalate into the clay layers and NaOH did not destroy the clay layered structure. The d_{001} spacing of Na-bentonite was 15.33 Å.

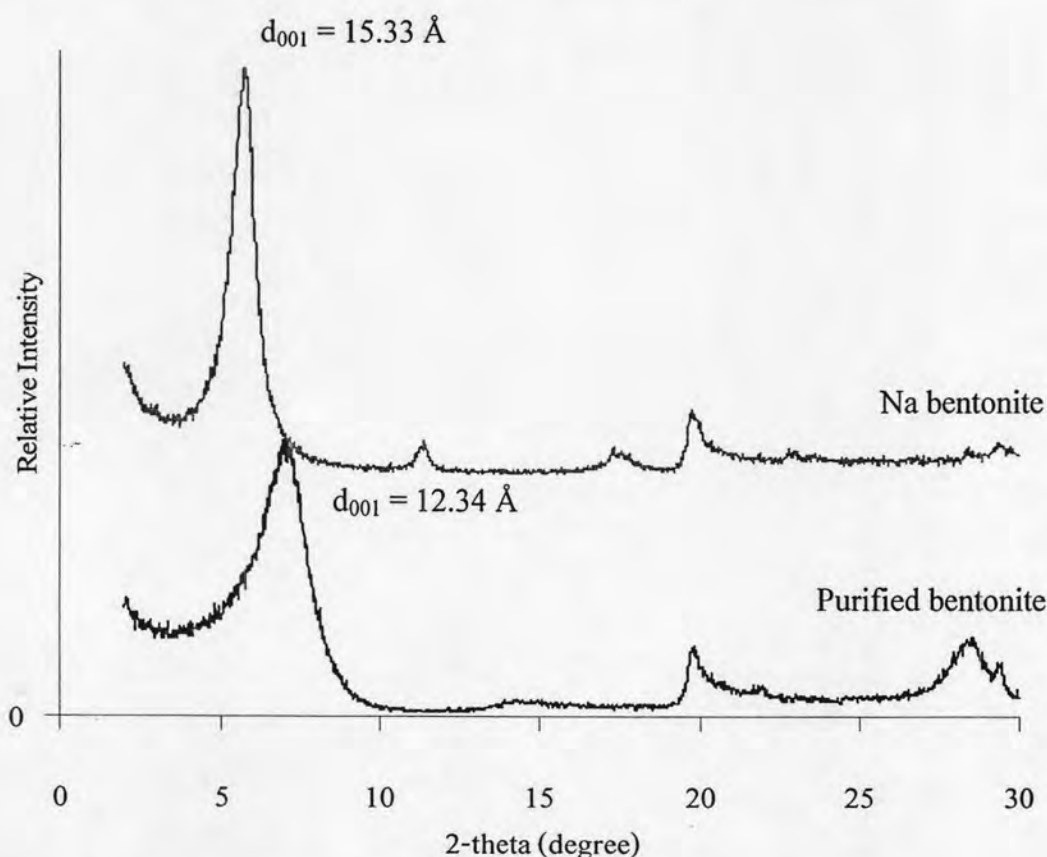


Figure 4.3 XRD patterns of purified bentonite and Na-bentonite.

4.3 The synthesis and characterization of Cu-pillared clays

Clay itself shows both Brønsted and Lewis acidity. By replacing the inter layer ions with high charge density cations like Al^{3+} , Zn^{2+} and Fe^{2+} , the strength and degree of acidity can be increased. According to Josept [39], Cu-pillared bentonite was synthesized by intercalation of copper precursors between the clay layers, following by calcinations at high temperature. The synthesized product (Cu-bentonite) was calcined at 300°C for 4 h. Cu-pillared bentonite as grey-brown solid was successfully synthesized.

4.3.1 X-ray diffraction of Cu-precursor intercalated clay layer

The XRD patterns of purified bentonite and Cu-intercalated bentonite are shown in Fig 4.4. The d_{001} reflection peak of Cu-pillared bentonite was shifted from 12.34 to 15.23 Å. The higher d_{001} spacing of Cu-pillared bentonite could be described by intercalation of copper polyoxocations between clay layers.

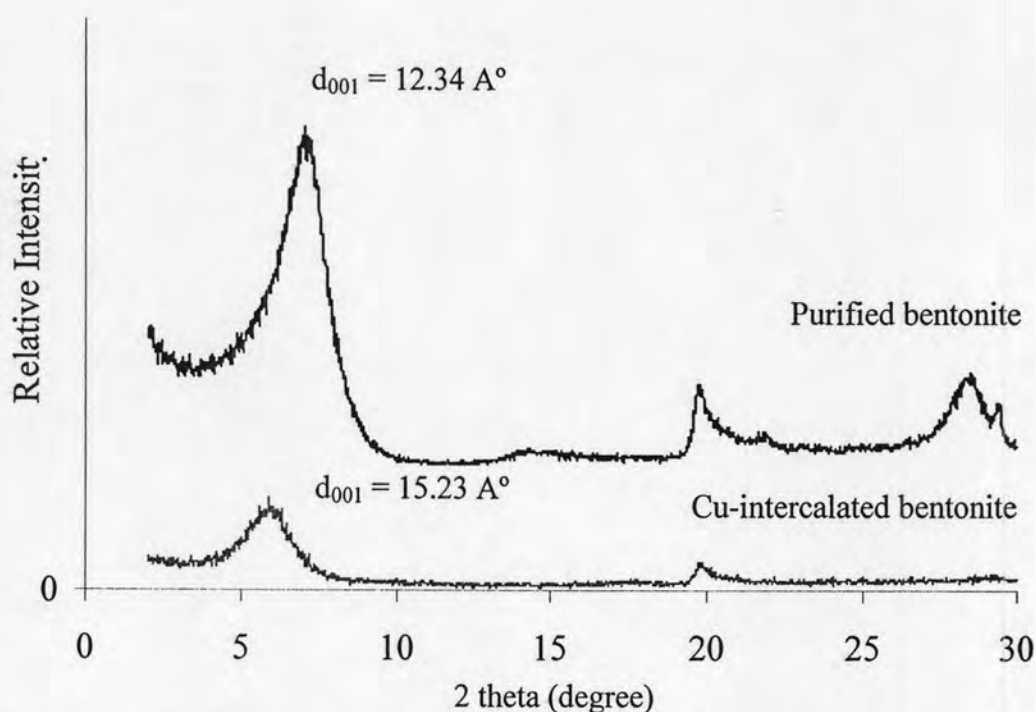


Figure 4.4 XRD patterns of purified bentonite and Cu-intercalated bentonite.

4.3.2 The characterization of Cu-pillared clays by XRD

Cu-intercalated bentonite was calcined at 300°C for 4 h. The XRD patterns of Cu-intercalated bentonite and Cu-pillared bentonite are shown in Fig 4.5. The d_{001} spacing of Cu-pillared bentonite was lower than that of Cu-intercalated bentonite. It can be explained that excess water adsorbed between clay layers was removed and the bulky copper precursors were converted to the pillars of copper oxide during calcination process.

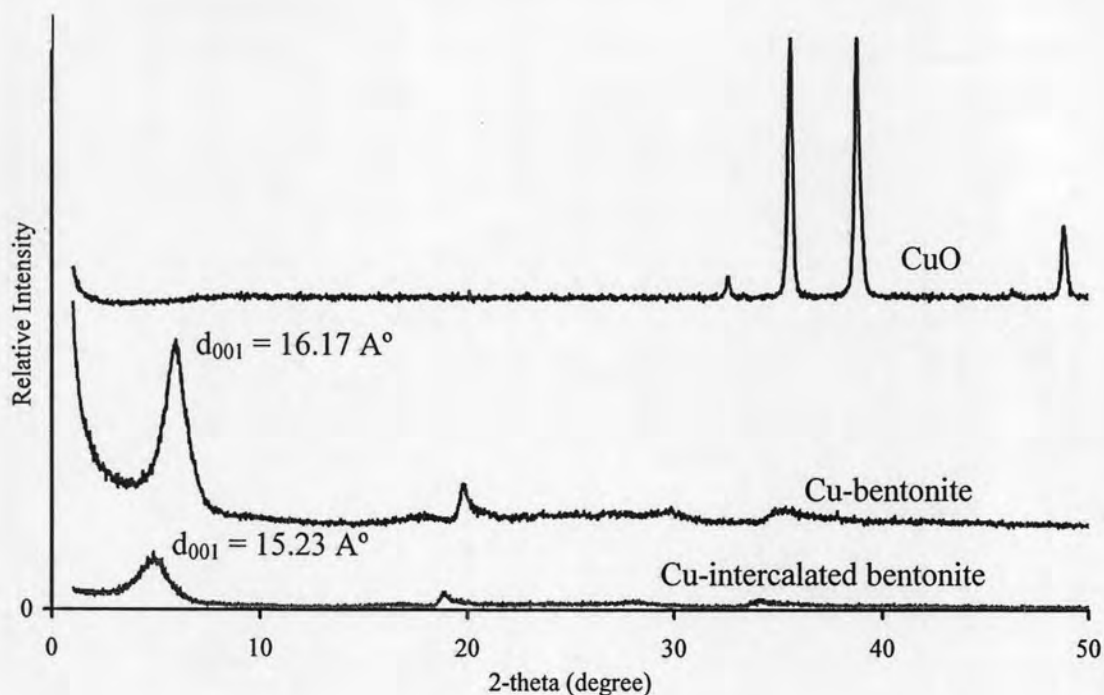


Figure 4.5 XRD patterns of CuO, Cu-bentonite and Cu-pillared bentonite.

4.3.3 Determination of copper contents

The copper content in Cu-pillared bentonite was analyzed by ICP method and compared with that of raw bentonite. Cu ion is not present in the chemical formula of pure montmorillonite, the active constituent of bentonite; however, as the natural clay, the transition metal impurities are normally found in bentonite. Thus, the copper content in Cu-pillared bentonite must be compared with that in the raw bentonite. Table 4.1 reports the copper contents in the form of CuO. The large amount of copper in Cu-pillared Bentonite, exceeding the cation exchanged capacity, suggests that copper would be in the pillared form within the interlayer. In addition, the XRD pattern of Cu-pillared bentonite shown in Fig. 4.5 contains no peak of copper oxide, which indicates no significant amount of copper oxide species outside the clay structure.

Table 4.1 The copper contents in clays sample

Samples	Wt% of CuO
Raw bentonite	1.85
Cu-pillared bentonite	15.59

4.3.4 The characterization of Cu-pillared clays by nitrogen adsorption-desorption (with Brunauer-Edmelt-Teller method, BET)

The surface area and pore type are very important in the catalytic application of materials since they reflect to the availability of the active sites towards the reactants. For the porous materials, the most widely used procedure to characterize the surface is BET analysis. The BET specific surface area of raw bentonite, Cu-pillared bentonite, and synthesized CuO are compared in Table 4.2. Their nitrogen adsorption-desorption isotherms are shown in Figs A-1 to A-3.

Table 4.2 The BET specific surface area of raw clays, Cu-pillared clays and CuO

Samples	BET specific surface area (m ² /g)
Raw bentonite	62.81
Cu-pillared bentonite	131.35
CuO	2.33

The nitrogen adsorption-desorption isotherms of Cu-pillared clays clearly demonstrated the distorted reversible type IV isotherm, indicating that CuO in the interlayer region converted clay-layered structure (2-dimensional structure) to mesoporous structure (3-dimensional structure) by connecting the adjacent aluminosilicate layers with the copper oxide pillars. Unlike highly crystalline materials such as zeolites, the pore structure of most metal oxide pillared clays is not uniformly distributed; however, the estimated value is still valid. The pore size distribution of Cu-pillared clays obtained from BJH analysis is in the range of 50 to 70 Å, indicating the group of mesoporous material (defined as having the diameter of 20-500 Å).

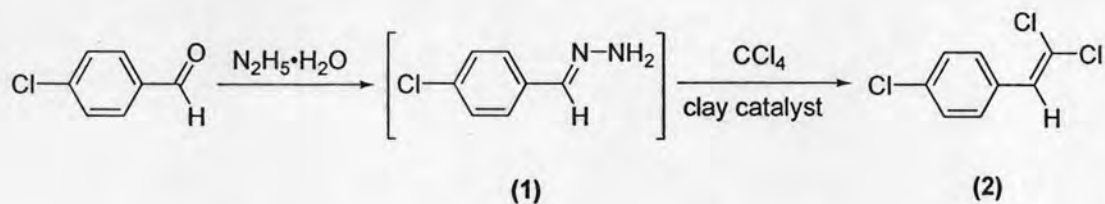
The surface area of the Cu-pillared bentonite is twice of that of bentonite. From the previous section, it was observed that the CuO content was increased by 13.74%; however, the surface of the bulk CuO was as low as a 2.33 m²/g. If the CuO in the prepared Cu-pillared bentonite is present as a bulk CuO outside the clay structure, the surface area would be lower than the bentonite. This result was also confirmed that CuO in the prepared Cu-pillared bentonite was distributed inside the interlayer of bentonite.

4.4 Catalytic activity of Cu-pillared clay in olefination of carbonyl compounds

In addition, olefination of carbonyl compounds was studied. Olefination of carbonyl compounds, *i.e.*, the conversion of C=O group into double C=C bond has found increasing application in the synthesis of substituted alkene [43]. Up to now, numerous olefination methods utilizing various reagents have been developed [43]. Among these, the Wittig reaction and its versions [7-9], Peterson reaction [10, 11] and Julia olefination [12, 13], are most widely in synthetic practice. However, these procedures require large amounts of organometallic compounds, and the reactions are carried out as a rule in an inert atmosphere in dry solvents. Therefore, the search for alternative methods for olefination of carbonyl compounds, specifically catalytic ones, remains an important problem.

Clay minerals occur abundantly in nature and their high surface area, sorptive and ion-exchange properties have been exploited for catalytic applications through decades. Solid clay catalysts [44] have a broad range of functions including use as catalytically active agents (as solid acids). Cation-exchanged clay possesses the ability to catalyze organic reaction [45]. During the 1930's and 40's, acid-treated clays were major catalysts used in petroleum processing, though they were later replaced by more thermostable zeolite. The modified clays are versatile heterogeneous catalysts for a wide variety of organic reaction.

Olefination of carbonyl compounds was selected for testing the catalytic activity of synthesized Cu-pillared clays. The reaction time, reaction temperature and the amount of catalyst were varied to search for the optimal conditions.



Hydrazone of 4-chlorophenylbenzaldehyde (1) was observed by reaction of 4-chlorobenzaldehyde and hydrazine hydrate in step 1 without intermediate isolation and carbontetrachloride was added to the above mixture. The product 1-(2,2-dichlorovinyl)-4-chlorobenzene (2) was observed.

4.4.1 Effect of bentonite and Cu-pillared clay catalysts on the reactivity of olefination of carbonyl compounds

The intercalation produces a large increase in the basal spacing of the clays, and the calcination transforms the intercalated polyoxocations into metal oxide clusters by dehydration and dehydroxylation processes. After calcination, the metal hydroxycations are converted to metal oxide (CuO) clusters acting as pillared that keep the clay layers apart and create interlayer and interpillar spaces, and thereby create a stable microporous system in the interlamellar space of clay particles. The catalytic activity of Cu-pillared bentonite was compared with copper oxide (CuO) and pure bentonite. The condition applied for the reaction was 30 wt% catalyst to aldehyde at RT (27°C) for 4 h. The results are presented in Table 4.3.

Table 4.3 Effect of various catalysts on the reactivity of olefination

Catalysts	% Isolated yield
None	0
Raw bentonite	0
Cu-pillared bentonite	72
CuO	34

Reaction conditions: aldehyde (0.01 mol), DMSO (5 mL), CCl₄ (0.05 mol)

Reaction time: step I at reflux for 3 h, step II at RT for 4 h.

When the reaction was performed without catalyst and raw clay, no product was observed. Thus, the transition metal catalyst is needed for this reaction. From Table 4.3, CuO showed lower activity than Cu-pillared bentonite. This result corresponds to the lower surface area of CuO. Cu-pillared bentonite has both the high copper content and large BET surface area, therefore it exhibited the most activity in olefination reaction of aldehyde to furnish dichlorostyrene (**2**) in high yield with excellent regioselectivity.

4.4.2 Study on the optimum conditions for olefination of carbonyl compounds by Cu-pillared bentonite

As shown in the previous section, Cu-pillared bentonite can be used as a catalyst for olefination reaction at first. The effect of the amount of catalyst and the reaction temperature on the outcome of the reaction were examined for the optimal condition.

Effect of the amount of catalyst on olefination of carbonyl compounds

The amount of catalyst normally influences the performance of the reaction. The variation of the amount of Cu-pillared bentonite on olefination reaction was carried out and the results are presented in Table 4.4.

Table 4.4 Effect of the amount of Cu-pillared bentonite on olefination of aldehyde

Entry	Cu-pillared bentonite	% Isolated yield
1	5 wt%	53
2	10 wt%	61
3	30 wt%	72
4	50 wt%	75
5	70 wt%	77

Reaction conditions: aldehyde (0.01 mol), DMSO (5 mL), CCl₄ (0.05 mol)

Reaction time: step I at reflux for 3 h, step II at reflux for 4 h.

According to the above results, the increase amount of catalyst assisted the production of the desired product derived from olefination reaction. It should be mentioned here that the high yield of **2** was achieved when 70 wt% of Cu-pillared bentonite to aldehyde was employed.

Effect of the reaction time and reaction temperature for Cu-pillared bentonite catalyzed on olefination reaction

The effect of the reaction time and reaction temperature on olefination reaction catalyzed by Cu-pillared bentonite was examined. The results are shown in Table 4.5.

Table 4.5 Effect of reaction time and reaction temperature for Cu-pillared bentonite catalyzed on olefination reaction

entry	time (h)	% Isolated yield	
		at RT	at reflux
1	2	50	52
2	4	72	73
3	6	78	78

Reaction conditions: aldehyde (0.01 mol), DMSO (5 mL), CCl₄ (0.05 mol), 30 wt% Cu-pillared bentonite to aldehyde

Reaction time: step I at reflux for 3 h., step II at reflux for 4 h.

Table 4.5 reveals that the olefination of aldehyde could be carried out at room temperature (27°C) by Cu-pillared bentonite furnishing the target product 72% within 4 h. The yield of **2** could be increased when the reaction time increased and reached 78% yield using 30 wt% Cu-pillared bentonite to aldehyde within 6 h. Furthermore, the reaction at reflux temperature (150°C) was investigated. The yield of **2** at reflux temperature were closed to those at room temperature at every reaction periods. The optimum time and temperature for this reaction are 4 h and room temperature respectively.

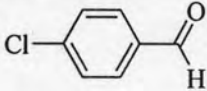
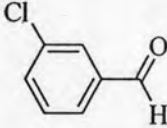
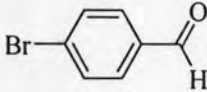
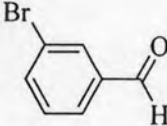
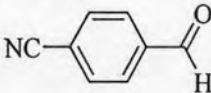
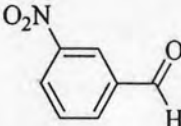
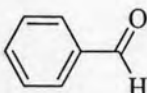
4.4.3 Application of developed procedures for the synthesis of target molecules

To investigate the generality and scope of this method, the reaction was carried out with various structurally diverse aldehydes and halogenated reagent. Condition for this reaction was 30% catalyst to aldehydes at room temperature (27°C) and reflux temperature (150°C) for 3 h in step 1 and 4 h for step 2

4.4.3.1 Effect of aldehydes

To test the generality of this method, the range of aldehydes were utilized in this developed procedure. These results are outlined in Table 4.6.

Table 4.6 Effect of type of aldehyde for Cu-pillared bentonite catalyzed on olefination reaction

Entry	Starting aldehyde	% Isolated yield	
		at RT	at reflux
1		72	74
2		53	55
3		69	66
4		60	62
5		68	-
6		61	62
7		25	26

Reaction conditions: aldehyde (10 mmol), DMSO 5 mL, CCl₄ 5 eq., Cu-bentonite 30wt%, 24 h.

Table 4.6 reveals that hydrazone (1) from step I could react with various aldehydes using Cu-pillared bentonite catalyst to furnish the desired products with different extents of yield. In order to improve the yield of target molecule, the system needed some modification such reaction temperature. Nevertheless, in case of performing the reaction at reflux temperature, the yield of the desired product was similar to that obtained at RT. Therefore the following study would concentrate on the reaction carried out at RT as the optimum condition in olefination of aldehydes.

The study on the effect of several substituents at *para*- position of aromatic ring provided some informative clues (entries 1, 3 and 5). The formation of alkenes were attained in high yield (72%, entry 1, 68%, entry 5 and 69%, entry 3, respectively). This may be because their negative charges in *para*- of aromatic ring was simply reacting with halogen group (-Cl, -Br). Thus, the more electron withdrawing group on aromatic ring presents, the higher yield was obtained. In the case of *meta*-position of aromatic ring (entries 2, 4 and 6), the desired alkene was attained in moderate yield (53%, entry 2, 60%, entry 4 and 61%, entry 6, respectively). From substituent effect, *meta*-directing groups are strongly deactivating group, resulting in providing less product. In addition, when the starting aldehyde was benzaldehyde, the desired alkene was achieved in only poor yield (25%, entry 7). This may result from no substituents on the aromatic ring.

All products could be fully characterized their identities by ^1H NMR.

The ^1H -NMR spectrum of 1-(2,2-dichlorovinyl)-4-chlorobenzene (Fig. 4.6) showed a singlet proton signal of an olefinic proton at δ_{H} 6.81. Four aromatic protons were observed from the presence of doublet ($J= 8.65$ Hz) signal at δ_{H} 7.48 and 7.46 and other doublet ($J= 8.65$ Hz) signals at δ_{H} 7.35 and 7.33, respectively.

The ^1H -NMR spectrum of 1-(2,2-dichlorovinyl)-3-chlorobenzene (Fig. 4.7) presented a singlet proton signal of an olefinic proton at δ_{H} 6.72. Other three aromatic protons were observed from the presence of triplet ($J= 7.17$ Hz) and doublet ($J= 6.54$ Hz) signal at δ_{H} 7.37 and 7.16, respectively. The singlet signal at δ_{H} 7.61 could be assigned for the aromatic proton between chloro- and dichloroalkene substituents.

The ^1H -NMR spectrum of 1-(2,2-dichlorovinyl)-4-bromobenzene (Fig. 4.8) revealed the singlet proton signal of an olefinic proton at δ_{H} 6.79. Four aromatic protons were observed from the presence of doublet ($J= 8.50$ Hz) signal at δ 7.50 and 7.49 and other doublets ($J= 8.42$ Hz) at δ_{H} 7.41 and 7.39, respectively.

The $^1\text{H-NMR}$ spectrum of 1-(2,2-dichlorovinyl)-3-bromobenzene (Fig. 4.9) displayed the singlet proton signal of an olefinic proton at δ_{H} 6.79. Other three aromatic protons were observed from the presence of triplet ($J= 7.67$ Hz) and doublet ($J= 7.93$ Hz) signals at δ_{H} 7.47 and 7.24, respectively. The singlet signal at δ_{H} 7.69 could be assigned for the aromatic proton located between bromo- and dichloroalkene substituents.

The $^1\text{H-NMR}$ spectrum of 4-(2,2-dichlorovinyl)-benzotrile (Fig. 4.10) presented the singlet proton signal of an olefinic proton at δ_{H} 6.81. Four aromatic protons were observed from the presence of doublet ($J= 8.62$ Hz) signal at δ_{H} 7.35 and 7.33 and other doublet ($J= 8.57$ Hz) signal at δ_{H} 7.48 and 7.46, respectively.

The $^1\text{H-NMR}$ spectrum of 1-(2,2-Dichlorovinyl)-3-nitrobenzene (Fig. 4.11) revealed that the singlet proton signal of an olefinic proton at δ_{H} 6.93. Other three aromatic protons were observed from the presence of the triplet ($J= 8.50$ Hz) and the doublet ($J= 7.89$ Hz) signals at δ_{H} 7.84 and 7.82 and the doublet ($J= 8.17$ Hz) signals at δ_{H} 8.18 and 8.16, respectively. The singlet signal at δ_{H} 8.73 could be assigned for aromatic proton which was between nitro- and dichloroalkene substituents.

The $^1\text{H-NMR}$ spectrum of 1-(2,2-dichlorovinyl)-benzene (Fig. 4.12) showed the singlet proton signal of an olefinic proton at δ_{H} 6.87. The signals around δ_{H} 7.36 were typical of three aromatic protons. Other two aromatic protons were observed from the presence of the doublet ($J= 7.32$ Hz) signals at δ_{H} 7.55 and 7.53.

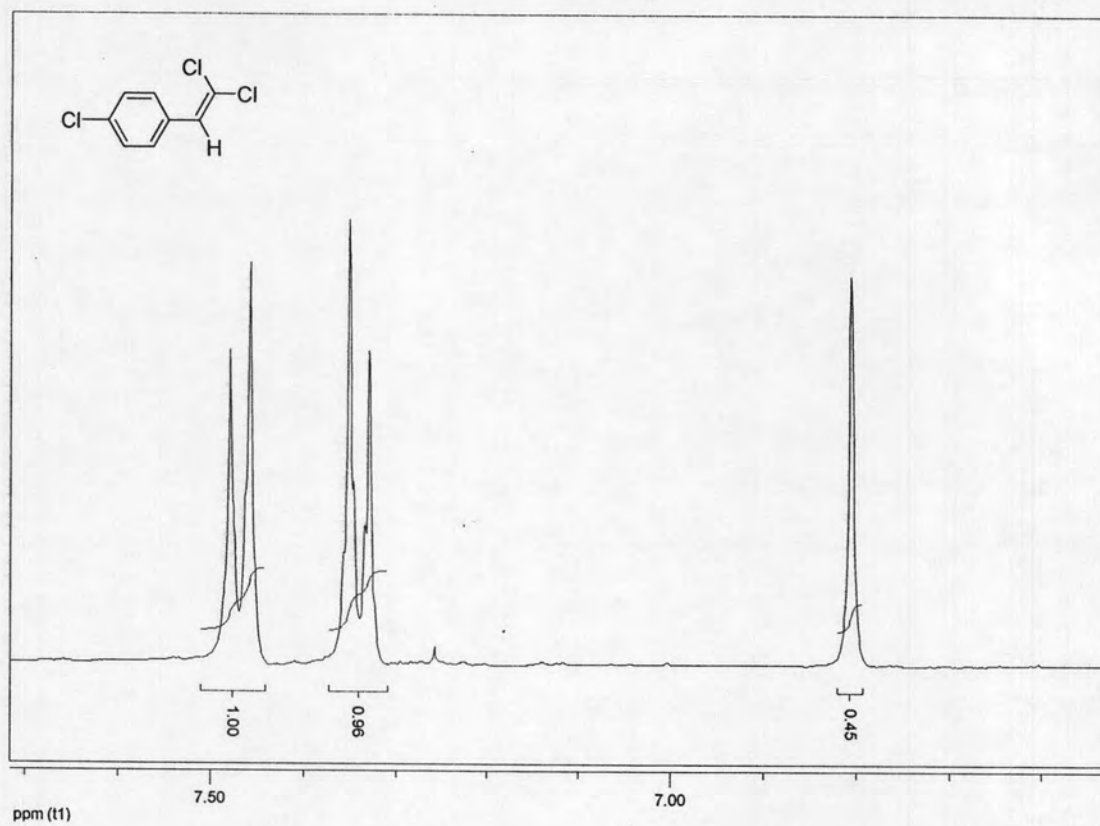


Figure 4.6 The ¹H-NMR spectrum of 1-(2,2-dichlorovinyl)-4-chlorobenzene.

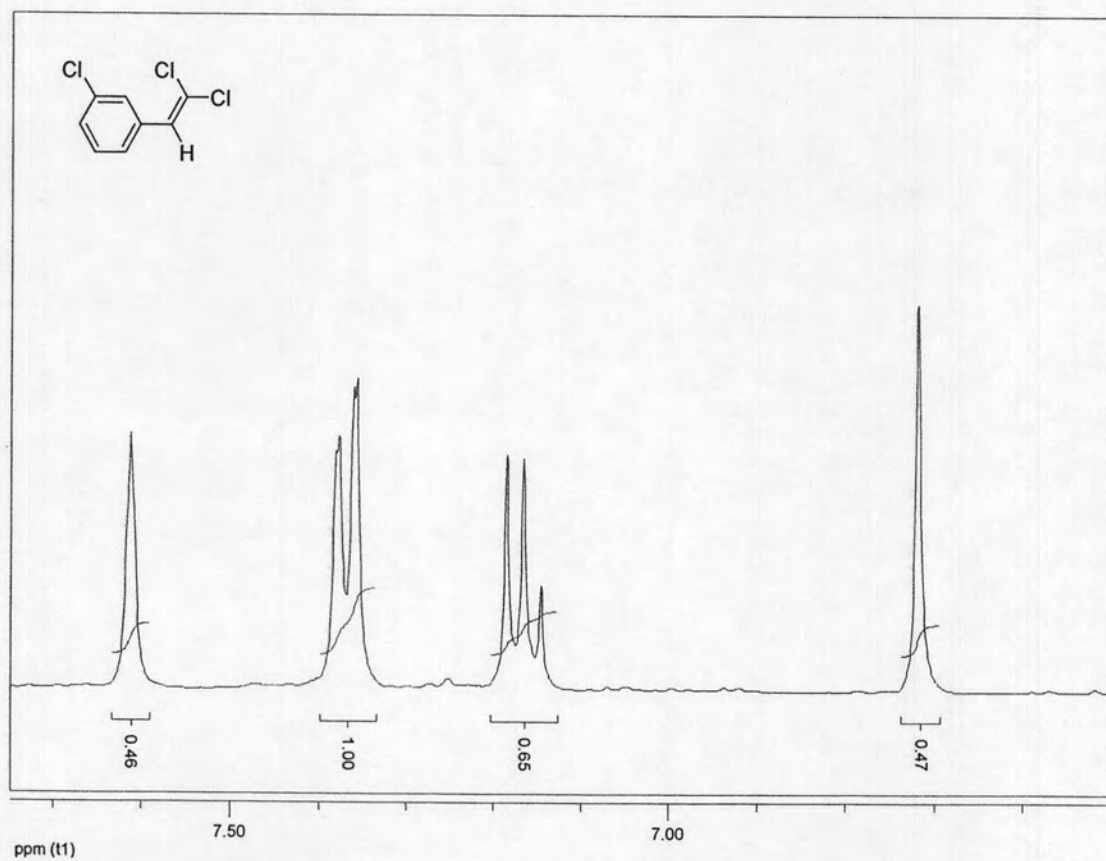


Figure 4.7 The ¹H-NMR spectrum of 1-(2,2-dichlorovinyl)-3-chlorobenzene.

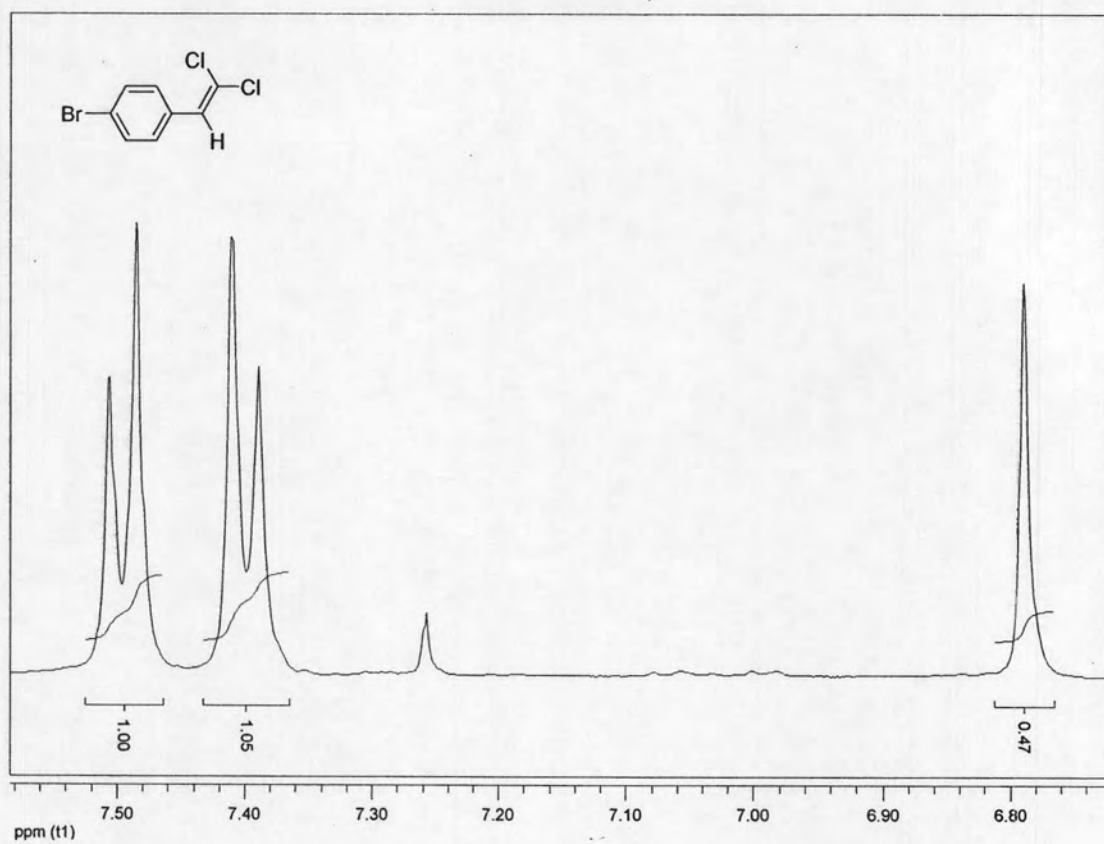


Figure 4.8 The ¹H-NMR spectrum of 1-(2,2-dichlorovinyl)-4-bromobenzene.

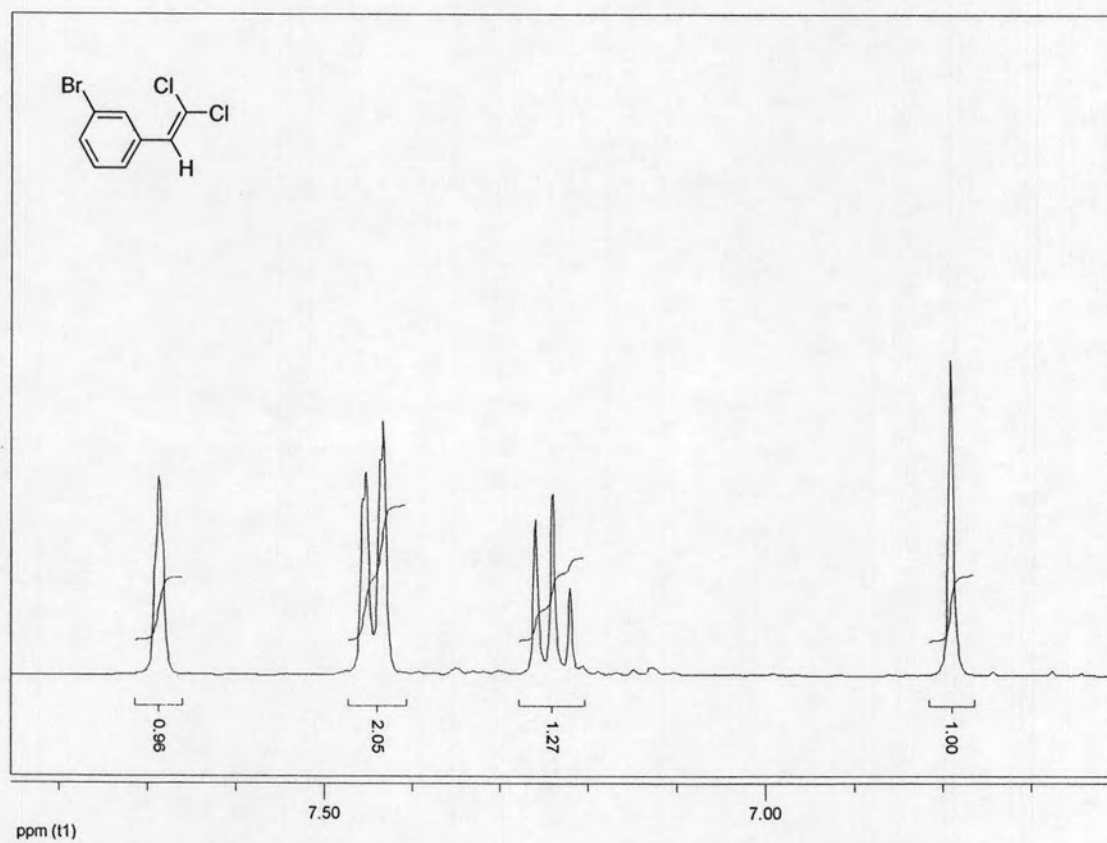


Figure 4.9 The ¹H-NMR spectrum of 1-(2,2-dichlorovinyl)-3-bromobenzene.

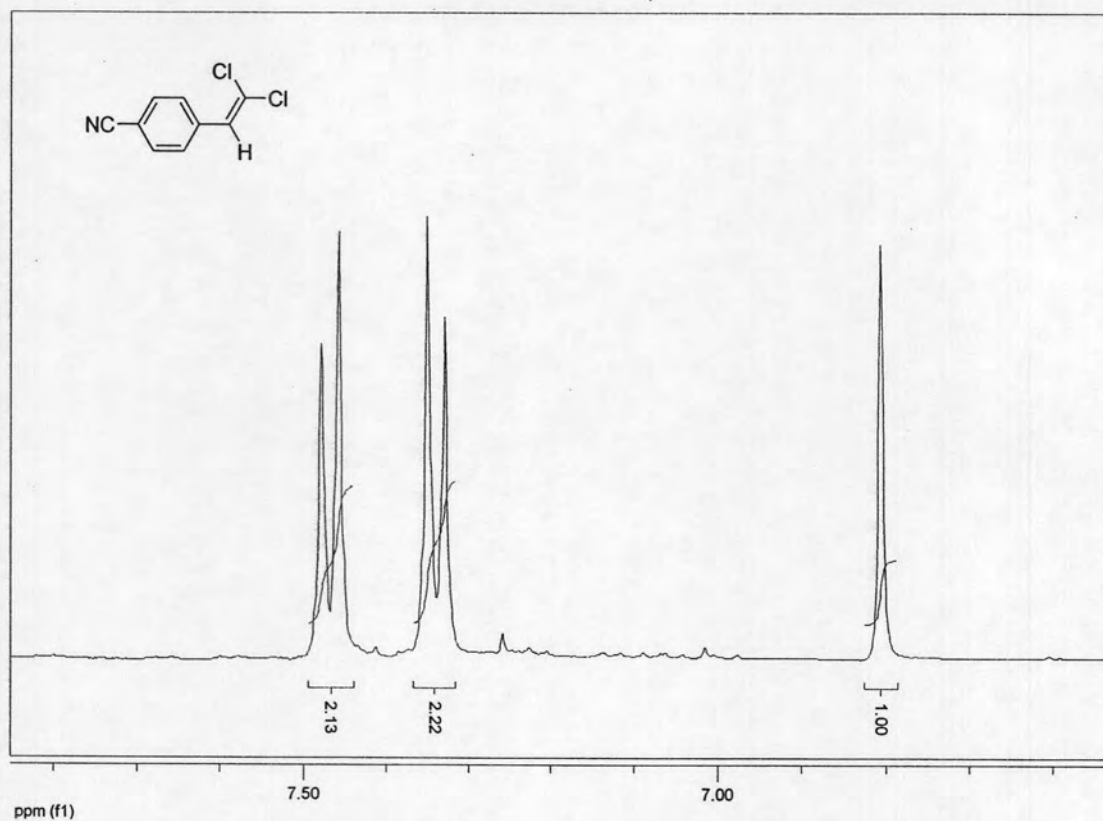


Figure 4.10 The ¹H-NMR spectrum of 4-(2,2-dichlorovinyl)benzonitrile.

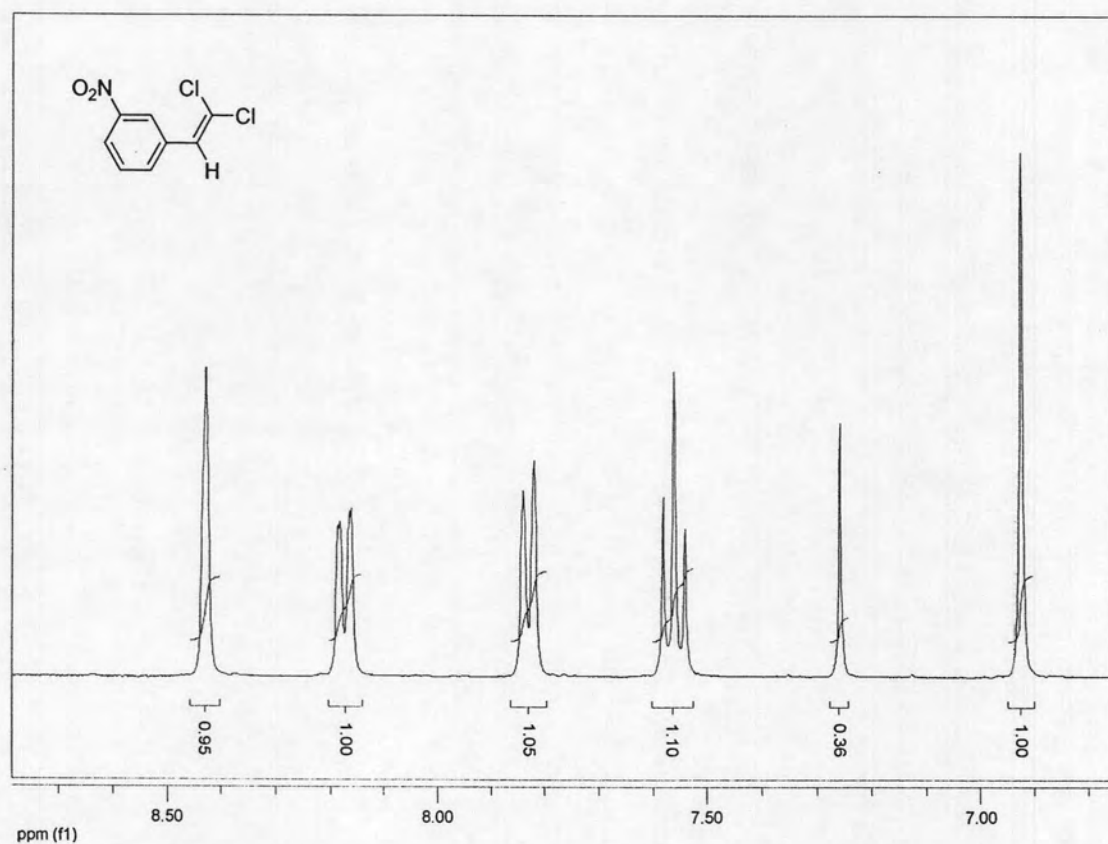


Figure 4.11 The ¹H-NMR spectrum of 1-(2,2-dichlorovinyl)-3-nitrobenzene.

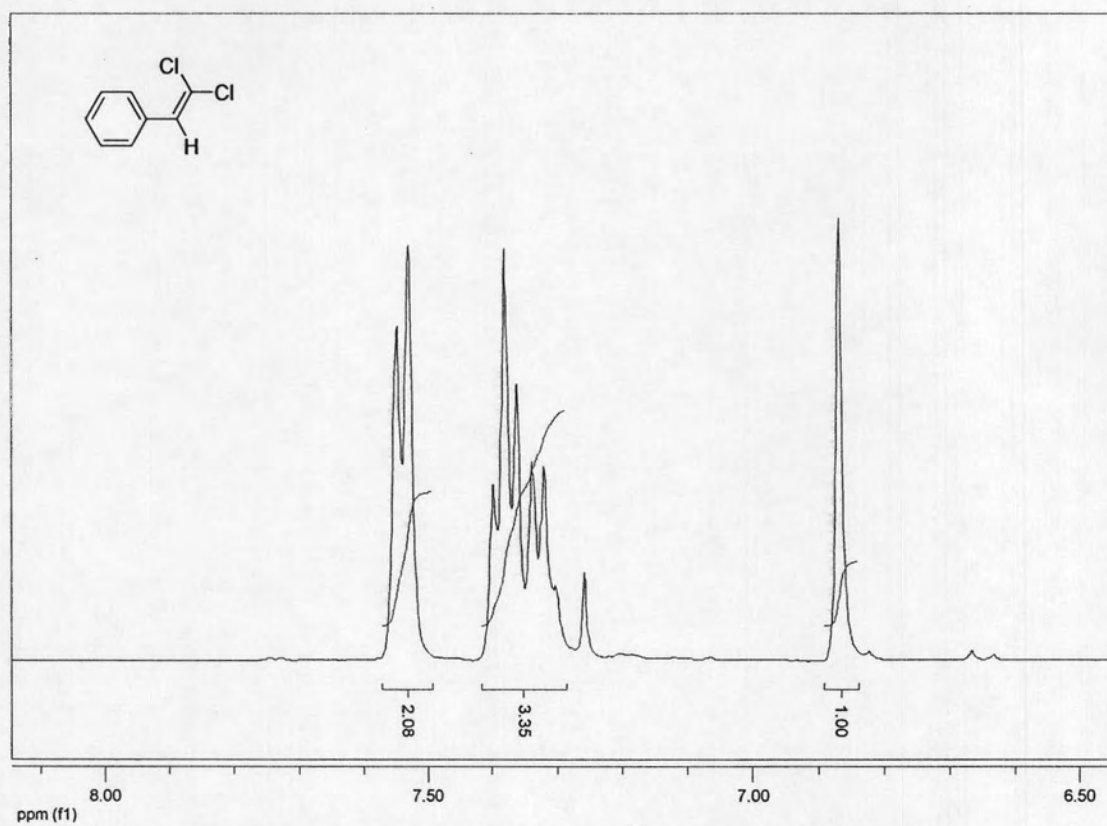
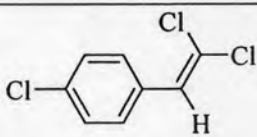
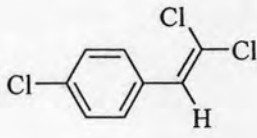
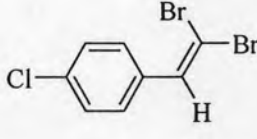
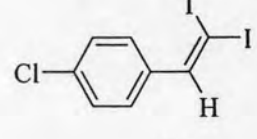
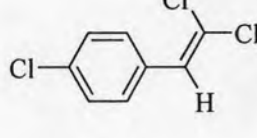


Figure 4.12 The $^1\text{H-NMR}$ spectrum of 1-(2,2-dichlorovinyl)-benzene.

4.4.3.2 Effect of halogenated reagent

The diverse ranges of halogenated reagents were then tested for this developed reaction. 4-Chlorobenzaldehyde was selected as a model substrate with a number of common halogenated reagents. The results of these reactions are summarized in Table 4.7.

Table 4.7 Effect of type of halogenated reagent

Entry	Halogenated reagent	Product	% Isolated yield
1	CCl ₄		72
2	CCl ₃ Br		71
3	CBr ₄		67
4	CHI ₃		trace
5	CCl ₃ F		trace
6	CH ₃ I	-	N/D
7	Cl ₃ C CONH ₂	-	N/D
8	CCl ₃ CN	-	N/D

Reaction conditions: aldehyde (10 mmol), DMSO 5 mL, CCl₄ 5 eq., Cu-pillared bentonite 30wt%, RT, 4 hr.

Table 4.7 reveals that other halogenated reagents such as CCl₃Br and CBr₄ could be used instead of CCl₄. The desired alkenes were achieved in high yield (71%, 67% for entries 2 and 3). The results suggest that the reactivities of such tetrahalomethanes as CBr₄ and CBrCl₃ be almost similar. The reactivity of these

compounds could be determined by the strength of the weakest C–Br bond which was broken first upon oxidative addition of the copper–carbene complex [46]. The copper atom within the complex was formally electron deficient in the absence of a C–Cl interaction. Donation of electron density from the two electrons of C–Cl σ bond to copper reduced to copper reduces this electron deficiency [47]. As applied to other halogenated reagents, the desired products were achieved in only poor yields (entries 4-5). Replacement of chlorine or bromine by fluorine and iodine increases the strength of the carbon–halogen bond. Introduction of electron-acceptor substituents led to an appreciable decrease in the energy of the C–Cl and C–Br bonds. However, when halogenated reagents such as CH_3I , $\text{Cl}_3\text{CCONH}_2$ and CCl_3CN were employed, the desired products were not obtained (entries 6-8). This may be due to the strength of the carbon–hydrogen bond. In the case of CCl_3CN (entry 8), the cyano group is more electronegativity than chlorine.

4.5 Regenerated catalysts

4.5.1 The characterization of the regenerated catalyst by XRD

The XRD patterns of Cu-pillared bentonite and the regenerated Cu-pillared bentonite are shown in Fig. 4.13.

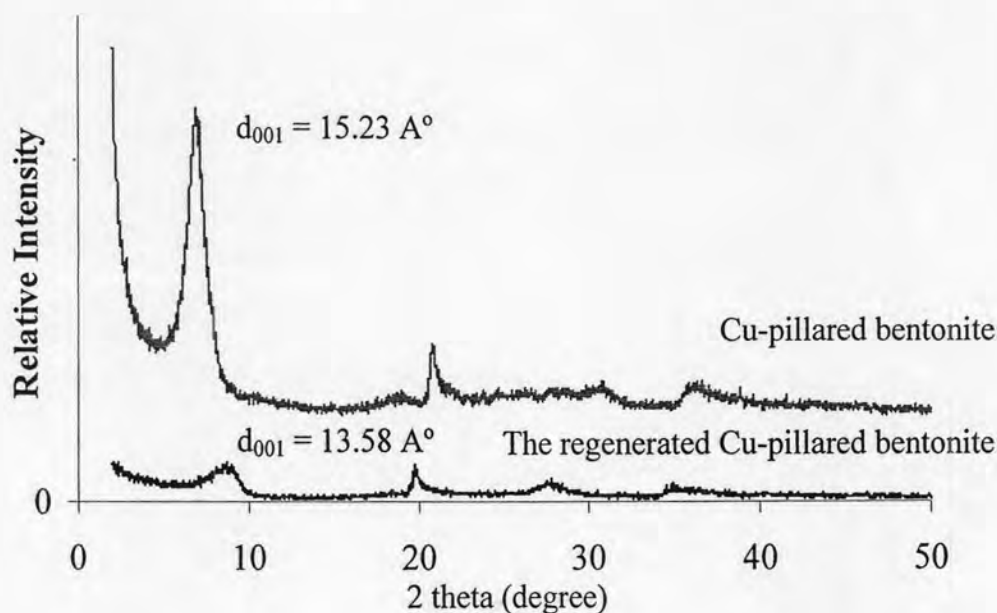


Figure 4.13 XRD patterns of Cu-pillared bentonite and the regenerated Cu-pillared bentonite.

After the olefination of carbonyl compounds, the clay catalyst was filtered from the reaction mixture and calcined at 300°C for 4 h in order to regenerate the catalyst. The d-spacing of regenerated Cu-pillared bentonite is lower than Cu-pillared bentonite (d_{001} 13.38 and 15.23); however, the characteristic pattern of clay remains, suggesting the collapse of the copper oxide pillars within the interlayers. The collapse may cause from the re-calcination process at high temperature and the local heat produced from the decomposition of organic species. The BET specific surface area of the regenerated catalyst, as shown in Table 4.8, is lower than the fresh one, corresponding to the said collapse. In addition, the re-calcination process at 300 °C is possible not enough to remove all organic residues, in which blocks the pores of pillared structure. However the specific surface area is still significantly larger than that of raw clay. The nitrogen adsorption-desorption isotherms of regenerated Cu-pillared bentonite is shown in Fig. A-4.

Table 4.8 The BET specific surface areas of raw bentonite, Cu-pillared bentonite and regenerated Cu-pillared bentonite

Samples	BET specific surface area (m ² /g)
Raw bentonite	62.81
Cu-pillared bentonite	131.35
Regenerated Cu-pillared bentonite	103.68

4.5.2 Catalytic activity of regenerated Cu-pillared bentonite in olefination of carbonyl compound

The regenerated Cu-pillared bentonite was used as a catalyst in olefination of 4-chlorobenzaldehyde with carbontetrachloride as a halogenated reagent. The results are summerized in Table 4.9.

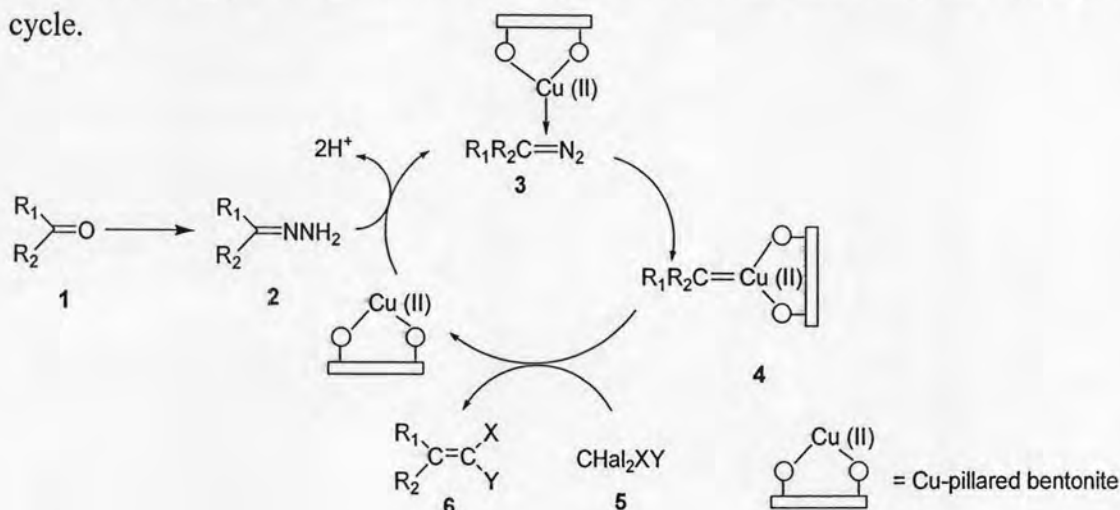
Table 4.9 Olefination of carbonyl compound catalyzed by regenerated Cu-pillared bentonite

Catalyst	% Isolate yield
Cu-pillared bentonite	72
regenerated Cu-pillared bentonite	68

Reaction conditions: aldehyde (10 mmol), DMSO 5 mL, halogenated reagent 5 eq., Cu-pillared bentonite 30wt%, RT, 24 hr.

Table 4.9 suggests that regenerated Cu-pillared bentonite can act as an efficient catalyst for olefination of carbonyl compound. In addition, the yield of regenerated Cu-pillared bentonite is a bit lower than Cu-pillared bentonite, corresponding to the result of the smaller d-spacing and the lower BET specific surface area.

The proposed of the catalytic cycle is describing catalytic olefination reaction (Scheme 4.1). In the first step, hydrazone (**2**) is oxidized by Cu-pillared bentonite to form the corresponding diazoalkane (**3**). The involvement diazoalkenes as intermediates of catalytic olefination reaction has reliably been proved earlier [48]. The subsequent copper-pillared bentonite catalyzed decomposition of diazoalkane (**3**) affords copper-carbene complex (**4**), which is the key intermediate of the reaction. The reaction of complex (**4**) with halogenated reagent (**5**) results in the corresponding dihaloalkenes (**6**) with regeneration of Cu-pillared bentonite and being a new catalytic cycle.



Scheme 4.1 Mechanism of olefination of carbonyl compounds catalyzed by Cu-pillared clay.